Journal of Muscle Research and Cell Motility (2023) 44:311–323
https://doi.org/10.1007/s10974-023-09660-6

ORIGINAL PAPER

The role of ZBP1 in eccentric exercise-induced skeletal muscle necroptosis

Kexin Shi[1] · Xiaoxue Wang[1] · Zhifei Ke[1] · Junping Li[1,2,3]

Received: 11 July 2023 / Accepted: 28 September 2023 / Published online: 27 October 2023

Abstract

This study aimed to explore the occurrence of necroptosis in skeletal muscle after eccentric exercise and investigate the role and possible mechanisms of ZBP1 and its related pathway proteins in the process, providing a theoretical basis for the study of exercise-induced skeletal muscle injury and recovery. Forty-eight male adult Sprague–Dawley rats were randomly divided into a control group (C, n = 8) and an exercise group (E, n = 40). The exercise group was further divided into 0 h (E0), 12 h (E12), 24 h (E24), 48 h (E48), and 72 h (E72) after exercise, with 8 rats in each subgroup. At each time point, gastrocnemius muscle was collected under general anesthesia. The expression levels of ZBP1 and its related pathway proteins were assessed using Western blot analysis. The colocalization of pathway proteins was examined using immunofluorescence staining. After 48 h of eccentric exercise, the expression of necroptosis marker protein MLKL reached its peak ($P < 0.01$), and the protein levels of ZBP1, RIPK3, and HMGB1 also peaked ($P < 0.01$). At 48 h post high-load eccentric exercise, there was a significant increase in colocalization of ZBP1/RIPK3 pathway proteins, reaching a peak ($P < 0.01$). (1) Eccentric exercise induced necroptosis in skeletal muscle, with MLKL, *p*-MLKL^{S358}, and HMGB1 significantly elevated, especially at 48 h after exercise. (2) After eccentric exercise, the ZBP1/RIPK3-related pathway proteins ZBP1, RIPK3, and *p*-RIPK3^{S232} were significantly elevated, particularly at 48 h after exercise. (3) Following high-load eccentric exercise, there was a significant increase in the colocalization of ZBP1/RIPK3 pathway proteins, with a particularly pronounced elevation observed at 48 h post-exercise.

Keywords ZBP1 · Exercise · Necroptosis · Skeletal muscle · MLKL

Introduction

Cell death is a fundamental pathological and physiological process underlying various diseases. Based on the type of death process, cell death can be classified into two major categories: programmed cell death (PCD) and non-programmed cell death. Among them, PCD is an essential component of organismal development and plays a critical role in host defense against pathogens and maintenance of cellular homeostasis.

Necroptosis, a type of programmed cell death, is a regulated cell death process controlled by receptor-interacting protein kinases (RIPKs) (Galluzzi and Kroemer 2008). Its hallmark features include cytoplasmic swelling, plasma membrane rupture, and release of cellular contents (Farber 1994). Necroptosis is implicated in various diseases, such as myocardial infarction (Khoury et al. 2020) and atherosclerosis (Moore and Tabas 2011; Karunakaran et al. 2016) in cardiovascular diseases, as well as Alzheimer's disease (Salvadores et al. 2022; Caccamo et al. 2017) and Parkinson's disease (Iannielli et al. 2018; Lin et al. 2020; Oñate et al. 2020) in neurological disorders. Necroptosis also plays a significant role in skeletal muscle diseases (Kamiya et al. 2022; Peng et al. 2022), yet research on the relationship between necroptosis and skeletal muscle-related diseases is scarce, and its underlying mechanisms remain unclear.

Z-DNA binding protein 1 (ZBP1) contains two N-terminal Z-DNA binding domains (ZBDs) (Zα1 and Zα2), two RIP homotypic interaction motif (RHIM) domains (RHIM1 and RHIM2), and one C-terminal signal domain (SD) (Jin

✉ Junping Li
doctorljp@126.com

[1] School of Human Sports Science, Beijing Sport University, Beijing, China

[2] Key Laboratory of Sports and Physical Health of Ministry of Education, Beijing Sport University, Beijing, China

[3] Present Address: Room 314, Teaching Laboratory Building, Beijing Sport University, Haidian District, No. 48, Xinxi Road, Beijing, China

et al. 2015). The N-terminal ZBDs enable ZBP1 to sense Z-DNA or other types of nucleic acid ligands, which is typically critical for ZBP1 activation (Wang et al. 2008; Ha et al. 2006, 2008; Kesavardhana et al. 2020); the interaction of ZBP1 with other RHIM-containing proteins forms the basis of signal transduction (Rebsamen et al. 2009; Kaiser et al. 2008; Muendlein et al. 2021). Additionally, the C-terminal region of ZBP1 is required for ZBP1-induced IFN-I response (Wang et al. 2008).

ZBP1 is a major regulatory factor in the induction pathway of necroptosis (Malireddi et al. 2019), and is involved in the induction and execution of necroptosis. Signal transduction of necroptosis involves four proteins carrying RHIM domains, namely ZBP1, RIPK1(Receptor-Interacting Serine/Threonine-Protein Kinase 1), RIPK3(Receptor-Interacting Serine/Threonine-Protein Kinase 3), and TRIF(TIR Domain-Containing Adaptor Protein Inducing Interferon-Beta) (Pearson et al. 2017). ZBP1 can interact with RIPK3 via the RHIM domain, which further activates MLKL(Mixed Lineage Kinase Domain-like Protein) and induces necroptosis. MLKL is a hallmark protein of necroptosis, and is activated by phosphorylation at different sites in different species in the necroptotic pathway (Al-Lamki et al. 2016; Rodriguez et al. 2016; Garcia et al. 2021; Kaiser and Offermann 2005). Ultimately, MLKL mediates signal transduction by binding to RIPK3, thereby determining the degree of necroptosis.

ZBP1 and its mediated ZBP1-RIPK3-MLKL pathway play significant roles in many human diseases (Karki et al. 2022; Baik et al. 2021), as well as various inflammatory processes (Devos et al. 2020), indicating a close relationship between ZBP1 and necroptosis. However, there are limited reports on the association between ZBP1 and exercise-induced skeletal muscle necroptosis, and the role of ZBP1 and its signaling pathway in this process remains to be elucidated. Therefore, this study focuses on ZBP1 as an entry point, and investigates the potential role and related mechanisms of necroptosis in skeletal muscle induced by eccentric exercise, in order to provide a theoretical basis for understanding the impact of exercise on skeletal muscle necroptosis and its underlying mechanisms.

Materials and methods

Animals

A total of 48 healthy male Sprague–Dawley (SD) rats, aged 8 weeks, were selected for the study. During the experimental period, the rats were provided with standard feed and had free access to water. Based on their body weights, the rats were randomly divided into two groups: a control group (C) and an exercise group (E). The exercise group (E) was further divided into different time intervals after exercise, including immediately after exercise (E0), 12 h after exercise (E12), 24 h after exercise (E24), 48 h after exercise (E48), and 72 h after exercise (E72), as shown in Table 1:

(1) Control group (C): Eight rats were raised under quiet conditions with free access to food and water, without any intervention.
(2) Exercise group (E): A single bout of high-intensity eccentric exercise was performed. Tissue samples were collected at the following time points: immediately after exercise(E0), 12 h after exercise(E12), 24 h after exercise(E24), 48 h after exercise(E48), and 72 h after exercise(E72). Each time point included 8 rats in the respective group. For the exercise group, the time point refers to the duration between the completion of exercise and tissue sampling.

Exercise protocols

All rats in Group E underwent a single bout of high-load eccentric exercise intervention, while Group C received no exercise intervention. Prior to formal training, an Adaptive Training was conducted to familiarize the animals with the environment and adapt to the training intensity. The specific implementation plan for the Adaptive Training was as follows: on Day 1, the treadmill incline was set at 0°, speed at 16 m/min, and exercise duration at 5 min; on Day 2, the treadmill incline remained at 0°, speed at 16 m/min, and exercise duration at 10 min; Days 3 and 4 were designated as rest days. On Day 5, formal training commenced with a single bout of high-load eccentric exercise. The training protocol followed the model of skeletal muscle damage induced by high-load eccentric exercise proposed by Armstrong et al. (1983). The

Table 1 Grouping information of experimental animals

Group Name	Control group	immediately after exercise	12 h after exercise	24 h after exercise	48 h after exercise	72 h after exercise
Name	C	E0	E12	E24	E48	E72

exercise was performed on an animal treadmill with a continuous downhill running protocol, featuring a treadmill incline of − 16°, speed of 16 m/min, and duration of 90 min. Detailed information is presented in Table 2.

Sample collection

The rats were weighed and anesthetized with an intraperitoneal injection of 25% urethane (6 ml/kg). The bilateral gastrocnemius muscles were rapidly dissected. A 3 × 3 × 5 mm sample was taken from each gastrocnemius muscle of each rat group, and the excess tendon and fascia were removed from the surface. The sample was wrapped in tin foil, labeled, and stored in a thermos with liquid nitrogen. A portion of the samples was placed in 4% paraformaldehyde that had been pre-cooled at 4 °C for fixation and kept at 4 °C for further testing. The remaining samples, after completion of sampling, were quickly transferred and stored at − 80 °C for further analysis.

Immunoblotting

The protein expression levels of ZBP1, RIPK3, *p*-RIPK3^{S232}, MLKL, *p*-MLKL^{S358}, and HMGB1 in rat skeletal muscle necroptosis were measured by Western blotting. The main steps were as follows: (1) protein extraction; (2) protein quantification; (3) gel preparation; (4) electrophoresis; (5) membrane transfer; (6) blocking; (7) primary antibody incubation: the concentrations of primary antibodies were as follows: ZBP1 (source: Rabbit, 1:1000), RIPK3 (source: Rabbit, 1:1000), MLKL (source: Rabbit, 1:2000), HMGB1 (source: Rabbit, 1:10,000), *p*-RIPK3^{S232} (source: Rabbit, 1:1000), *p*-MLKL^{S358} (source: Rabbit, 1:500), and GAPDH (source: Mouse, 1:2000); (8) membrane washing; (9) secondary antibody incubation: the concentrations of secondary antibodies were as follows: ZBP1 (Goat anti-rabbit IgG, 1:2000), RIPK3 (Goat anti-rabbit IgG, 1:2000), MLKL (Goat anti-rabbit IgG, 1:2000), HMGB1 (Goat anti-rabbit IgG, 1:2000), *p*-RIPK3^{S232} (Goat anti-rabbit IgG, 1:4000), *p*-MLKL^{S358} (Goat anti-rabbit IgG, 1:4000), and GAPDH (Goat anti-mouse IgG, 1:2000); (10) membrane washing; (11) exposure using an optical luminescence system; and (12) band analysis. Detailed information of the reagent is provided in Table 3.

Table 2 Exercise Training Program

Exercise mode	Days	Slope	Speed	Exercise duration
Adaptive training	Day 1	0°	16 m/min	5 min
	Day 2	0°	16 m/min	10 min
	Day 3	Rest		
	Day 4			
Formal training	Day 5	−16°	16 m/min	90 min

Immunofluorescence

(1) Sectioning; (2) Slide mounting; (3) Baking the slides; (4) Deparaffinization; (5) Antigen retrieval; (6) Application of tissue fluorescence quenching solution A; (7) Permeabilization; (8) Blocking; (9) Incubation with primary antibodies: ZBP1 (source: Rabbit, 1:100), RIPK3 (source: Mouse, 1:100), MLKL (source: Rabbit, 1:100); (10) Incubation with secondary antibodies: Goat Anti-Rabbit IgG H&L/AF555(1:200), Goat Anti-Mouse IgG H&L/AF488(1:200); (11) Nuclear staining; (12) Application of tissue fluorescence quenching solution B; (13) Slide sealing; (14) Image acquisition. Detailed information of the reagent is provided in Table 4.

Statistical analysis

The experimental images obtained from immunoblotting were quantitatively analyzed using Image J to obtain gray-scale values by analyzing the bands. For immunofluorescence images, Image J was utilized to perform quantitative analysis of co-localization between two fluorescence proteins and calculate the Pearson's coefficient between them. All data were statistically analyzed and graphed using SPSS

Table 3 Experimental reagents in immunoblotting

Reagent name	Manufacturer and product number
Anti-ZBP1 antibody	BIOSS/bs-13559R
Anti-RIPK3 antibody	Cell Signaling Technology/101,885
Anti-MLKL antibody	Abcam/ab243142
Anti-HMGB1 antibody	Abcam/ab79823
Anti- *p*-RIPK3^{S232} antibody	Affinity/AF7443
Anti- *p*-MLKL^{S358} antibody	Biorbyt /orb453305
Anti-GAPDH antibody	ZSGB-BIO/TA-08
Goat Anti-rabbit IgG	ZSGB-BIO/ZB-2301
Goat Anti-mouse IgG	ZSGB-BIO/ZB-2305

Table 4 Experimental Reagents in Immunofluorescence

Reagent name	Manufacturer and product number
Anti-ZBP1 antibody	BIOSS/bs-13559R
Anti-RIPK3 antibody	Abbexa/abx174349
Anti-MLKL antibody	Affinity/DF7412
Goat Anti-Rabbit IgG H&L/AF555	BIOSS/bs-0295G-AF555
Goat Anti-Mouse IgG H&L/AF488	BIOSS/bs-0296G-AF488

26.0 and GraphPad Prism 9 software. Data are expressed as mean ± standard deviation (SD). One-way ANOVA was used for intergroup comparisons, and LSD or Tamhane's T2 test was used for post-hoc comparisons, depending on the homogeneity of variance. A P-value < 0.05 was considered statistically significant, and a P-value < 0.01 was considered highly significant.

Results

Changes in skeletal muscle MLKL and p-MLKL^{S358} protein expression at different time points after eccentric exercise

As shown in Fig. 1, the overall trend of MLKL protein expression in rat skeletal muscle after a single bout of high-load eccentric exercise was characterized by an initial increase followed by a decrease, with the peak occurring at 48 h post-exercise. Compared with the control group, MLKL protein expression was significantly elevated at 48 and 72 h post-exercise ($P < 0.01$), with increases of 77.2% and 71.1%, respectively. The expression level began to decrease after 72 h post-exercise.

The overall pattern of p-MLKL^{S358} protein expression in skeletal muscle after a single bout of high-load eccentric exercise was characterized by a "wave-like" trend (An initial increase, followed by a decrease, then a subsequent increase, and finally a gradual decrease), with the peak occurring at 48 h post-exercise (Fig. 1). Compared with the control group, p-MLKL^{S358} protein expression was significantly increased at 48 h post-exercise ($P < 0.01$), with an increase of 56.5%.

Changes in skeletal muscle HMGB1 protein expression at different time points after high-load eccentric exercise

As shown in Fig. 2, the overall trend of HMGB1 protein expression in rat skeletal muscle after a single bout of high-load eccentric exercise was characterized by an initial increase followed by a decrease, with the peak occurring at 48 h post-exercise. Compared with the control group, HMGB1 protein expression was significantly increased at 12, 24 and 48 h post-exercise ($P < 0.05$ or $P < 0.01$), with increases of 51.8%, 61%, and 90%, respectively.

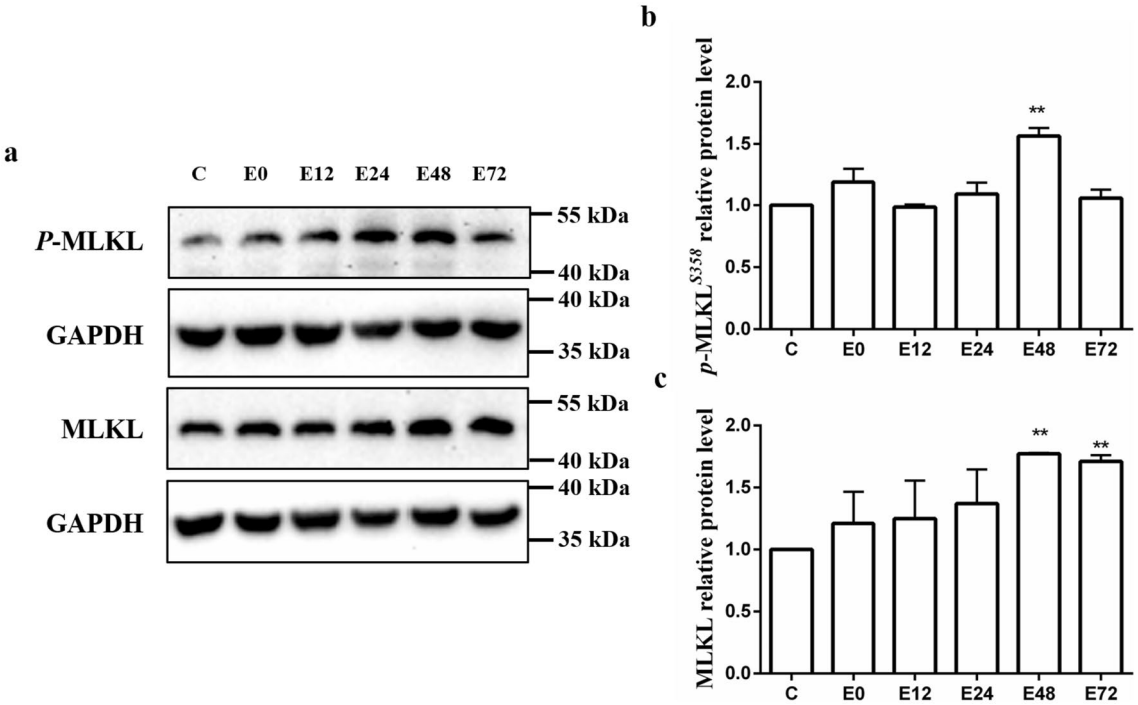

Fig. 1 Changes in skeletal muscle MLKL and p-MLKL^{S358} protein expression at different time points after eccentric exercise. The expression levels of p-MLKL^{S358} and total MLKL were analysed by immunoblotting (**a**) and quantified based on the loading control (GAPDH; quantification depicted in a histogram in **b** and **c**). While overall MLKL expression appears to increase following eccentric exercise, a two-wave response can be observed for p-MLKL^{S358}. Values are means ± SD. *$P < 0.05$, **$P < 0.01$ compared with the control group. For a comprehensive table comparing all the quantifications, please refer to the Supplementary Material

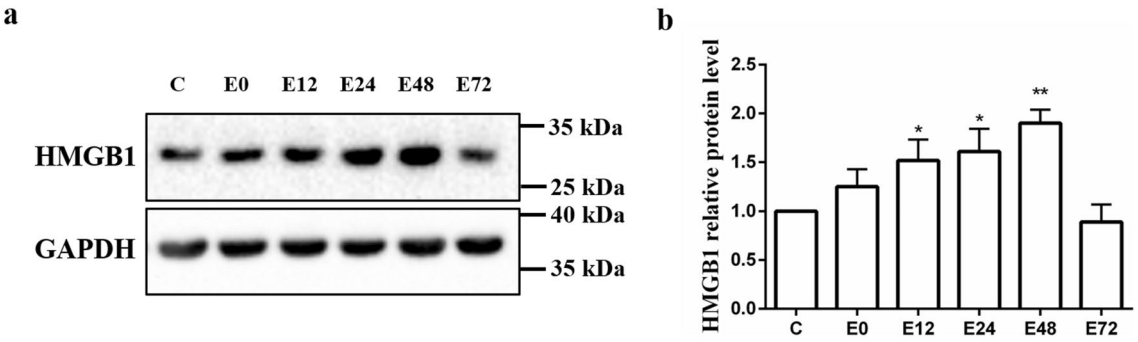

Fig. 2 Changes in skeletal muscle HMGB1 protein expression at different time points after eccentric exercise. The expression levels of HMGB1 were analysed by immunoblotting (**a**) and quantified based on the loading control (GAPDH; quantification depicted in a histogram in **b**). The overall trend of HMGB1 protein expression showed a gradual increase following eccentric exercise, with the peak occurring at 48 h post-exercise. Values are means ± SD. *$P < 0.05$, **$P < 0.01$ compared with the control group. For a comprehensive table comparing all the quantifications, please refer to the Supplementary Material

Changes in skeletal muscle ZBP1 protein expression at different time points after high-load eccentric exercise

As shown in Fig. 3, the overall pattern of ZBP1 protein expression in rat skeletal muscle after a single bout of high-load eccentric exercise was characterized by a "wave-like" trend (An initial decrease, followed by an increase, then a subsequent decrease, another increase, and finally a gradual decline), with the peak occurring at 48 h post-exercise. Compared with the control group, ZBP1 protein expression was significantly elevated at 48 and 72 h post-exercise ($P < 0.01$), with increases of 88% and 80.7%, respectively.

Changes in skeletal muscle RIPK3 and p-RIPK3^{S232} protein expression at different time points after high-load eccentric exercise

As shown in Fig. 4, the overall trend of RIPK3 protein expression in rat skeletal muscle after a single bout of high-load eccentric exercise was characterized by an initial increase followed by a decrease, with the peak occurring at 48 h post-exercise and gradually declining by 72 h. Compared with the control group, RIPK3 protein expression was significantly increased at 24, 48, and 72 h post-exercise ($P < 0.01$), with increases of 64.1%, 121.9%, and 64%, respectively.

The trend of *p*-RIPK3^{S232} protein expression was similar to that of RIPK3 (Fig. 4). The overall pattern of *p*-RIPK3^{S232} protein expression in rat skeletal muscle after a single bout of high-load eccentric exercise was characterized by an initial increase followed by a decrease, with the peak occurring at 48 h post-exercise, followed

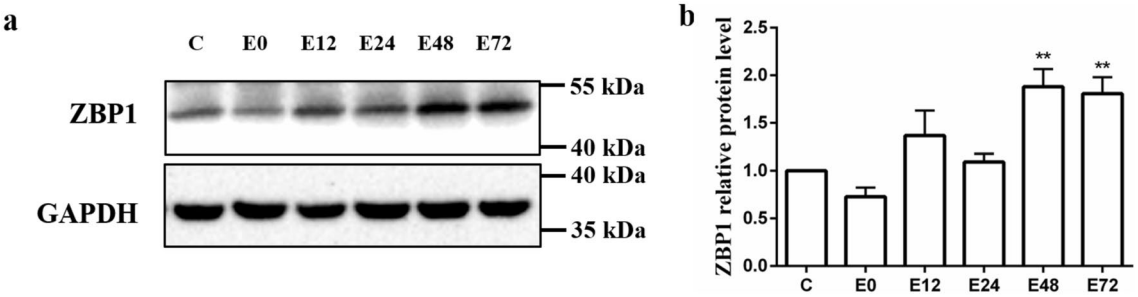

Fig. 3 Changes in skeletal muscle ZBP1 protein expression at different time points after eccentric exercise. The expression levels of ZBP1 were analysed by immunoblotting (**a**) and quantified based on the loading control (GAPDH; quantification depicted in a histogram in **b**). The overall expression pattern of ZBP1 protein exhibited a "wave-like" trend, characterized by an initial decrease, followed by an increase, then another decrease, subsequent increase, and finally a gradual decline. The peak expression occurred at 48 h post-exercise. Values are means ± SD. *$P < 0.05$, **$P < 0.01$ compared with the control group. For a comprehensive table comparing all the quantifications, please refer to the Supplementary Material

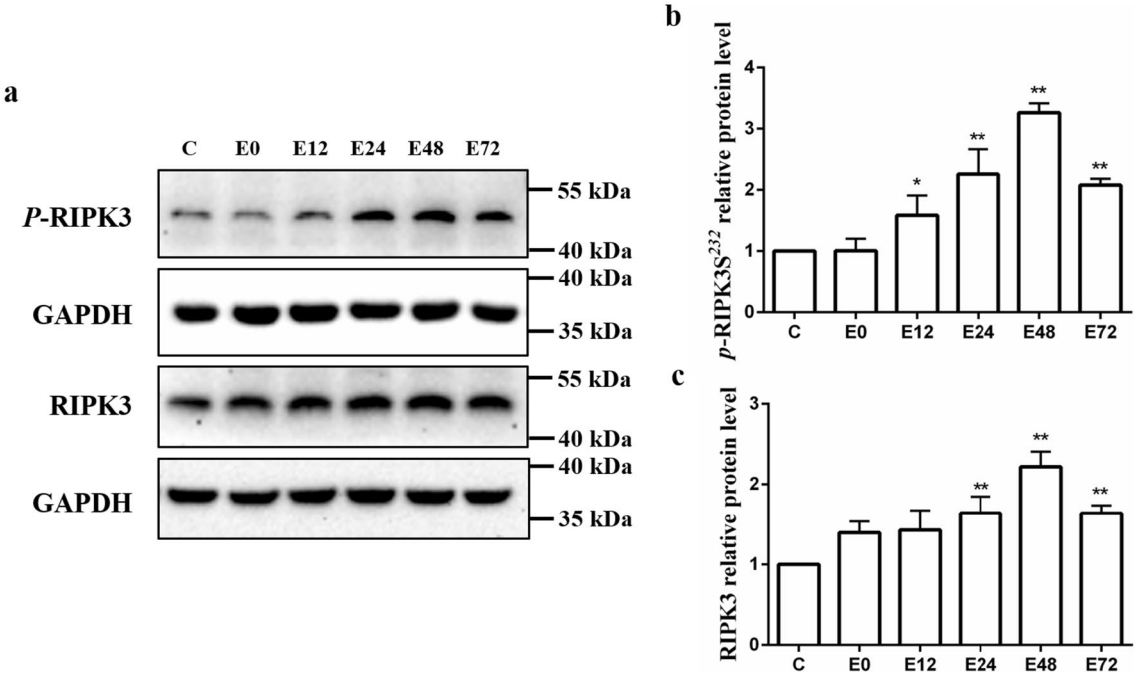

Fig. 4 Changes in skeletal muscle RIPK3 and *p*-RIPK3^{S232} protein expression at different time points after eccentric exercise. The expression levels of phosphorylated RIPK3 and total RIPK3 were analysed by immunoblotting (**a**) and quantified based on the loading control (GAPDH; quantification depicted in a histogram in **b** and **c**). The expression trend of *p*-RIPK3^{S232} protein was similar to that of RIPK3. Both *p*-RIPK3^{S232} and RIPK3 proteins exhibited an overall pattern of initial increase followed by a decrease. The peak expression occurred at 48 h post-exercise. Values are means ± SD. *$P < 0.05$, **$P < 0.01$ compared with the control group. For a comprehensive table comparing all the quantifications, please refer to the Supplementary Material

by a gradual decline. Compared with the control group, *p*-RIPK3^{S232} protein expression was significantly elevated at 12, 24, 48, and 72 h post-exercise ($P < 0.05$ or $P < 0.01$), with increases of 58.6%, 125.8%, 226.2%, and 108%, respectively.

Changes in the colocalization of ZBP1 and RIPK3 in skeletal muscle at different time points after high-load eccentric exercise

As shown in Fig. 5, ZBP1 is displayed in red fluorescence, while RIPK3 is displayed in green fluorescence. The colocalization of ZBP1 and RIPK3 is shown as yellow fluorescence. In the control (C) group, minimal colocalization was observed in the immunofluorescence images, whereas different levels of colocalization were observed in the immunofluorescence images at different time points after high-load eccentric exercise. The colocalization of ZBP1 and RIPK3 exhibited an overall increasing trend followed by a decrease, reaching a peak at 48 h post-exercise. Compared to the C group, the colocalization coefficient of ZBP1 and RIPK3 started to increase immediately after exercise, and it was significantly increased at 24 h, 48 h, and 72 h post-exercise ($P < 0.01$).

Changes in the colocalization of RIPK3 and MLKL in skeletal muscle at different time points after high-load eccentric exercise

As shown in Fig. 6, the immunofluorescence images show RIPK3 in green fluorescence and MLKL in red fluorescence. The colocalization of the two appears as yellow fluorescence. Minimal yellow colocalization was observed in the immunofluorescence images of the control (C) group, while different levels of colocalization were observed at different time points after high-load exercise. The colocalization coefficient of RIPK3 and MLKL exhibited an overall increasing trend followed by a decrease, reaching a peak at 48 h post-exercise. Compared to the C group, the colocalization coefficient of RIPK3 and MLKL started to increase immediately after exercise and was significantly increased at 24 h, 48 h, and 72 h post-exercise ($P < 0.05$ or $P < 0.01$).

Discussion

In previous studies, necrosis was considered a passive and unregulated form of cell death (Kaiser et al. 2013). However, in recent years, a new type of programmed cell death (PCD), namely necroptosis, has been reported and

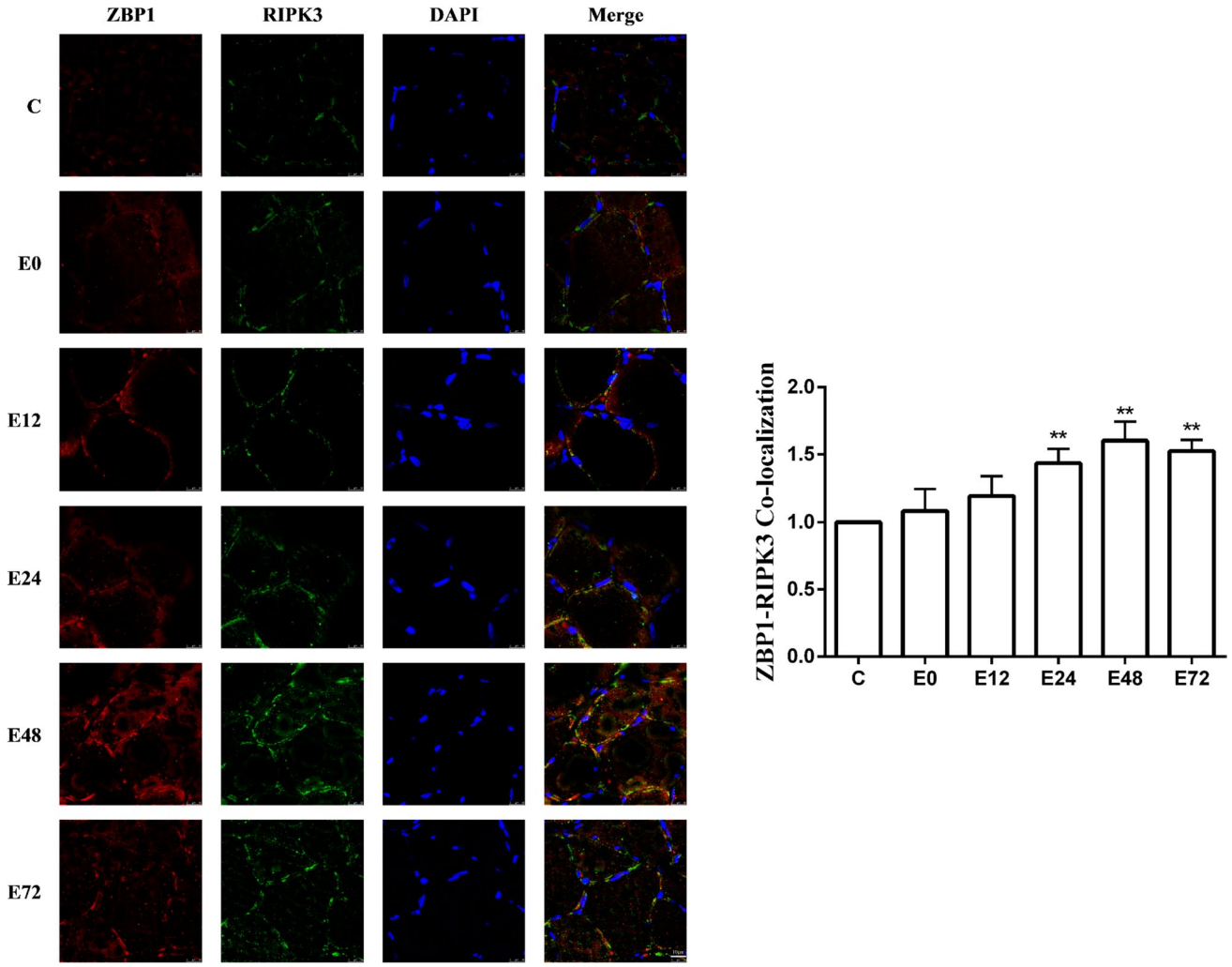

Fig. 5 Changes in the colocalization of ZBP1 and RIPK3 in skeletal muscle at different time points after high-load eccentric exercise (Scale Bar = 10 μm). Values are means ± SD. $^{*}P < 0.05$, $^{**}P < 0.01$ compared to the control (C) group

gradually attracted the attention of many scholars (Samir et al. 2020; Wang and Kanneganti 2021; Christgen et al. 2020; Jiao et al. 2020). PCD, as a normal physiological phenomenon in organism life activities, mainly includes apoptosis, autophagy, pyroptosis, and necroptosis. Necroptosis is regulated by related molecules, including RIPK1 and RIPK3 (Kuriakose et al. 2016; Ofengeim and Yuan 2013; Udawatte and Rothman 2021; Gurung et al. 2014), and is characterized by cytoplasmic swelling, plasma membrane rupture, and release of cellular contents (Farber 1994). Necroptosis occurs when the signal is transmitted downstream, activating the key signal protein MLKL, which induces p-MLKL protein to "punch holes" in the cell membrane, leading to the release of high mobility group box 1 (HMGB1) protein and ultimately mediating necroptosis (Chen et al. 2019).

The canonical pathway of necroptosis is mediated by TNF and is similar to the pathway mediated by ZBP1, both of which are regulated by RIPK1, RIPK3, and MLKL (Fritsch et al. 2019; Man et al. 2013; Henry and Martin 2017), as shown in Fig. 7. In the TNF pathway, RIPK1 promotes the auto-phosphorylation and activation of RIPK3. In contrast, in ZBP1-mediated necroptosis, ZBP1 directly induces the auto-phosphorylation of RIPK3. However, RIPK1 often acts as a negative regulator of necroptosis in the ZBP1 pathway, inhibiting necroptosis (Devos et al. 2020; Ingram et al. 2019; Newton et al. 2016).

Previous research has explored the potential mechanisms through the TNF pathway, but currently, there are few reports on the ZBP1-mediated signaling pathway for exercise-induced skeletal muscle necroptosis, and the role of ZBP1 and its signaling pathway in this process remains to be clarified.

In ZBP1-mediated necroptosis, ZBP1 directly induces the autophosphorylation of RIPK3. RIPK3 serves as the "initiator" of necroptosis, and ZBP1 induces the phosphorylation of RIPK3, thereby mediating the ZBP1-RIPK3-MLKL

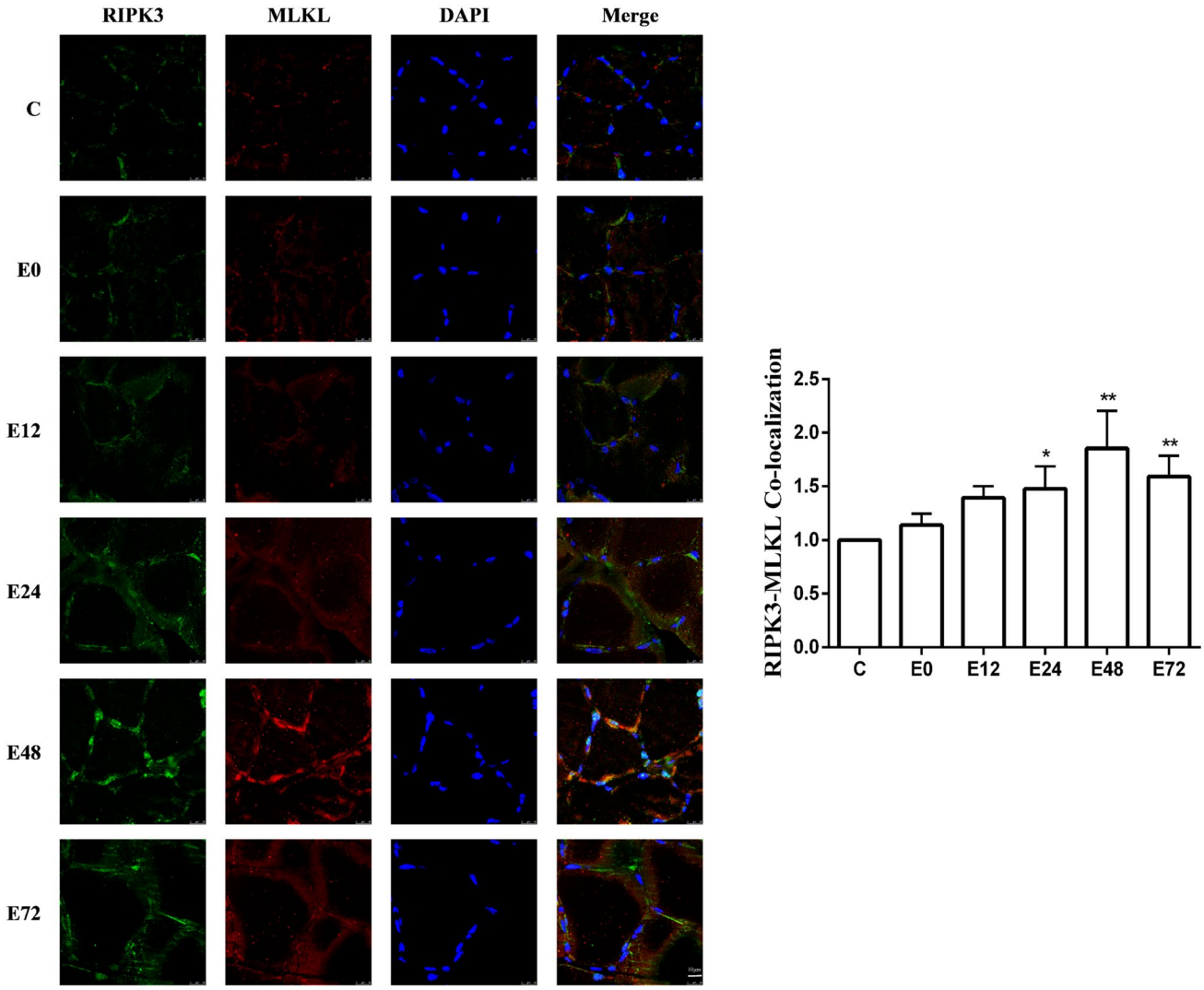

Fig. 6 Changes in the colocalization of RIPK3 and MLKL in skeletal muscle at different time points after high-load eccentric exercise (Scale Bar = 10 μm). Values are means ± SD. *$P < 0.05$, **$P < 0.01$ compared to the control (C) group

pathway. MLKL, on the other hand, acts as the "executioner" of necroptosis. RIPK3 phosphorylates MLKL, leading to the translocation of MLKL oligomers to the cell membrane and their subsequent pore formation. This process results in the release of inflammatory factors, such as HMGB1, ultimately triggering necroptosis (Xia et al. 2020; Mizumura et al. 2016; Xue et al. 2020).

Studies have shown that MLKL plays a crucial role in necroptosis. MLKL is a cytoplasmic protein consisting of 471 amino acids, which is widely distributed in various tissues or organs, such as the brain, liver, lung, myocardium, skeletal muscle, skin, and adipose tissue (Martens et al. 2021; Murphy et al. 2013). It has been reported that MLKL, as the "executioner" of necroptosis, not only has the potential to positively regulate the occurrence of necroptosis, but also can phosphorylate itself, leading to the formation of oligomers and pore formation on the cell membrane, which can promote the opening of Ca^{2+} or Na^{+} channels, resulting in membrane rupture, release of cellular contents, and induction of necroptosis (Kamiya et al. 2022). Increasing evidence suggests that the activation of MLKL at the S358/S345 sites is regarded as the "gold standard" for the occurrence of necroptosis and has been widely used in many in vivo and in vitro experiments (Meng et al. 2015; Li et al. 2017; Ito et al. 2016; Peltzer et al. 2018).

In the past 10–20 years, MLKL has been considered as the exclusive "executioner" of current necroptosis. However, as research has advanced, scholars have gradually discovered that MLKL can interact with other forms of programmed cell death (PCD). The occurrence of necroptosis is not linear or uniform as described but rather intricate and complex. Essentially, it can not only influence other regulated cell

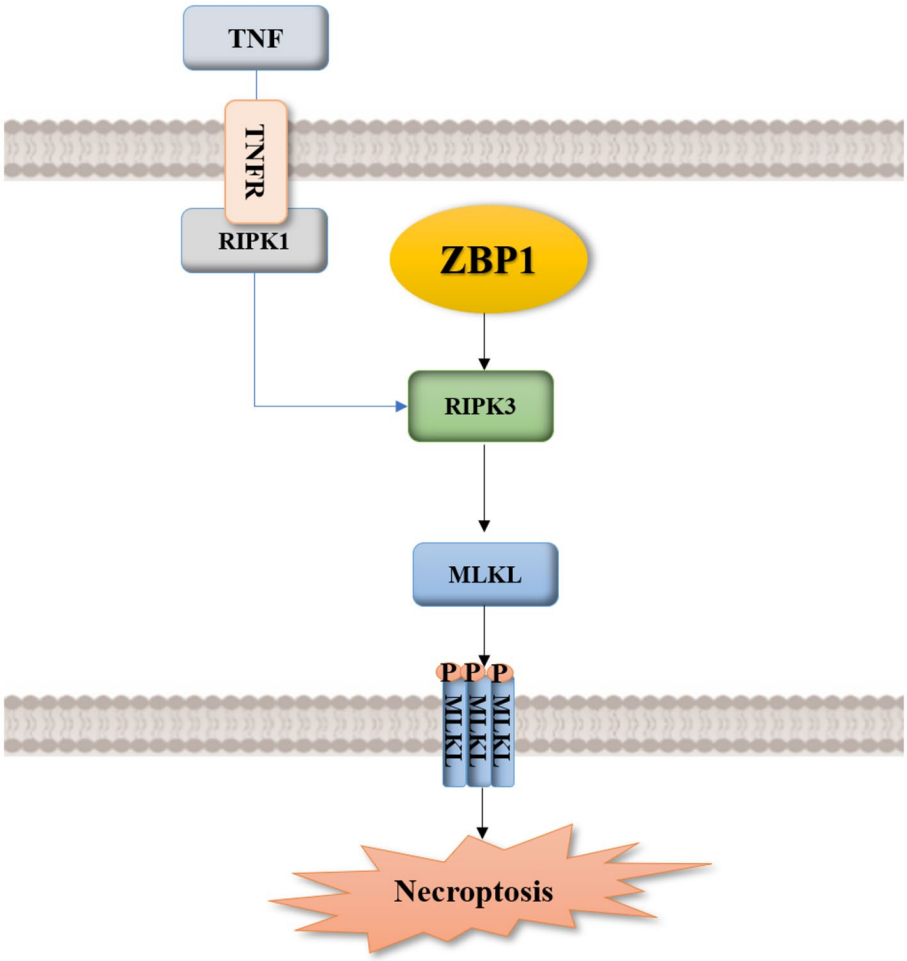

Fig. 7 The pathway of ZBP1 in necroptosis

death (RCD) processes or death-associated pathways but other RCD or death-associated pathways can also regulate necroptosis (Schwarzer et al. 2020). This suggests that the "cross-talk" between these cellular death pathways not only demonstrates the complexity of RCD but also indicates that MLKL possesses multiple biological functions. Apart from its involvement in necroptosis, MLKL is also involved in various other events such as autophagy, apoptosis, NLRP3 inflammasome activation, NETosis, and more (Zhan et al. 2021).

To further investigate whether eccentric exercise can induce necroptosis in rat skeletal muscle, based on previous studies, we measured the protein expression of MLKL and p-MLKL^{S358} to further confirm the occurrence of necroptosis at the protein level. We found that the overall expression of MLKL protein in rat skeletal muscle exhibited a trend of first increasing and then decreasing after high-load eccentric exercise at different time points, with significant increases at 48 h and 72 h after exercise ($P < 0.01$), and reaching the peak at 48 h. The expression of p-MLKL^{S358} protein also exhibited a "wave-like" trend (First increasing, then decreasing, then increasing again, and gradually decreasing thereafter), with a significant increase (56.5%) and the peak appearing at 48 h after exercise ($P < 0.01$), followed by a gradual decrease at 72 h. These results suggest that a single bout of high-load eccentric exercise may induce necroptosis in rat skeletal muscle.

One typical feature of necroptosis is the release of cellular contents, which was detected by immunoblotting analysis of the expression of the inflammation-related factor HMGB1 protein. We found that the overall expression of HMGB1 protein in rat skeletal muscle exhibited a trend of first increasing and then decreasing after a single bout of high-load eccentric exercise at different time points, with significant increases at 12 h, 24 h, and 48 h after exercise ($P < 0.05$ or $P < 0.01$). The peak expression was observed at 48 h after exercise, followed by a gradual decrease. Therefore, the results of this study indicate that a single bout of high-load eccentric exercise can lead to the release of cellular contents, further confirming the occurrence of necroptosis.

To date, there have been no reports on the ZBP1/RIPK3 pathway in high-load eccentric exercise. In this study, we used immunoblotting analysis to detect the protein expression of the ZBP1/RIPK3 pathway. For ZBP1, we found

that the overall expression of ZBP1 protein in rat skeletal muscle exhibited a "wave-like" trend after a single bout of high-load eccentric exercise at different time points (First decreasing, then increasing, then decreasing again, then increasing again, and gradually decreasing thereafter), with the peak expression observed at 48 h after exercise. Compared to the control group, the expression of ZBP1 protein was significantly increased at 48 h and 72 h after exercise ($P < 0.01$), with an increase of 88% and 80.7%, respectively. The expression gradually decreased after 72 h but remained significantly higher than the control group ($P < 0.01$). Additionally, we found that the expression trend of RIPK3 and p-RIPK3^{S232} was similar. After a single bout of high-load eccentric exercise, the overall expression of RIPK3 and p-RIPK3^{S232} proteins in rat skeletal muscle showed a trend of first increasing and then decreasing. The peak expression of RIPK3 was observed at 48 h after exercise, and the expression gradually decreased after 72 h. Compared to the control group, the expression of RIPK3 protein was significantly increased at 24 h, 48 h, and 72 h after exercise ($P < 0.01$), with increases of 64.1%, 121.9%, and 64%, respectively. The expression gradually decreased after 72 h but remained significantly higher than the control group ($P < 0.01$). The expression of p-RIPK3^{S232} gradually increased immediately after exercise and reached its peak at 48 h, followed by a gradual decrease. Compared to the control group, the expression of p-RIPK3^{S232} protein was significantly increased at 12 h, 24 h, 48 h, and 72 h after exercise ($P < 0.05$ or $P < 0.01$), with increases of 58.6%, 125.8%, 226.2%, and 108%, respectively. The expression gradually decreased after 72 h but remained significantly higher than the control group ($P < 0.01$). The observed "wave-like" trend in ZBP1 expression is speculated to be potentially influenced by other proteins or pathways that impact protein expression. For instance, RIPK1 protein (Devos et al. 2020; Ingram et al. 2019; Newton et al. 2016), which has been mentioned as a negative regulatory factor in the pathway mediated by ZBP1 and involved in necroptosis, could contribute to this phenomenon. As a suggestion for future research, this also implies that interference with relevant pathways, such as knockdown of certain key molecules, could be employed to further investigate their roles in necroptosis.

A single bout of high-load eccentric exercise generates mechanical pressure, resulting in muscle damage. It is also known that prolonged exercise duration is accompanied by metabolic stress, which can further contribute to muscle damage. Therefore, in subsequent studies on the mechanisms of skeletal muscle injury, it is important to consider that exercise not only induces mechanical pressure but also triggers metabolic stress. Thus, the wave-like trend of ZBP1 expression may potentially be attributed to a second hit caused by injury-induced inflammation. One characteristic feature of necroptosis is the release of cellular contents, and HMGB1 serves as both an inflammatory mediator and an indicator of cell membrane integrity (Mishra et al. 2019). By performing immunoblot analysis to assess the protein expression of the inflammatory factor HMGB1, we observed significant expression following a single bout of high-load eccentric exercise. Hence, after a single bout of high-load eccentric exercise, both mechanical pressure and metabolic stress are generated. The wave-like trend of ZBP1 expression may possibly be attributed to a second hit caused by injury-induced inflammation. There is a limitation in this study. It would have been more meaningful to simultaneously perform measurements on both the control group and the exercise group at the same time intervals after exercise. However, due to constraints in sample collection, this was not feasible.

Through immunofluorescence analysis, we observed that in the ZBP1/RIPK3 pathway, the colocalization coefficient of ZBP1 and RIPK3 proteins exhibited an overall increasing trend followed by a decrease, reaching a peak at 48 h post-exercise. Significant increases were observed at 24 h, 48 h, and 72 h post-exercise ($P < 0.01$). Notably, the colocalization trend between RIPK3 and MLKL proteins in this pathway was similar to that of ZBP1 and RIPK3. Furthermore, the expression of ZBP1, RIPK3, and MLKL proteins was upregulated. These findings suggest that the ZBP1/RIPK3 pathway in skeletal muscle is activated following a single bout of high-load eccentric exercise.

In summary, high-load eccentric exercise induced the occurrence of necroptosis in skeletal muscle. The necroptosis markers, MLKL and p-MLKL^{S358}, significantly increased at 48 h after exercise, and the release of cellular content protein HMGB1 also peaked at 48 h after exercise. Moreover, following high-load eccentric exercise, the ZBP1/RIPK3-related pathway proteins are activated, leading to an increase in protein colocalization within the pathway, thereby mediating the occurrence of necroptosis. In the future, it would be possible to further investigate the role of this pathway in necroptosis by interfering with relevant pathways and knocking out specific key molecules. These studies would provide a theoretical basis for understanding the impact of exercise on necroptosis in skeletal muscle and its underlying mechanisms.

Supplementary Information The online version contains supplementary material available at https://doi.org/10.1007/s10974-023-09660-6.

Author contributions KS, XW, ZK, and JL collectively conceived and designed the entire study; KS and XW conducted the experiments and analyzed the data; KS drafted the manuscript; JL, ZK, and XW reviewed and edited the manuscript. We thank all the participants for their contributions to the project.

Funding This work was supported by the Special Funded Project of the Basic Scientific Research Operation Fee of the Central University [Grant Nos. 2019PT013].

Data Availability The data used in this study are available upon request. Researchers interested in accessing the data can contact shikexin0611@126.com for further information.

Declarations

Competing interests The authors declare no competing interests.

References

Al-Lamki RS, Lu W, Manalo P, Wang J, Warren AY, Tolkovsky AM, Pober JS, Bradley JR (2016) Tubular epithelial cells in renal clear cell carcinoma express high RIPK1/3 and show increased susceptibility to TNF receptor 1-induced necroptosis. Cell Death Dis 7:e2287. https://doi.org/10.1038/cddis.2016.184

Armstrong RB, Ogilvie RW, Schwane JA (1983) Eccentric exercise-induced injury to rat skeletal muscle. J Appl Physiol Respir Environ Exerc Physiol 54:80–93. https://doi.org/10.1152/jappl.1983.54.1.80

Baik JY, Liu Z, Jiao D, Kwon HJ, Yan J, Kadigamuwa C, Choe M, Lake R, Kruhlak M, Tandon M, Cai Z, Choksi S, Liu ZG (2021) ZBP1 not RIPK1 mediates tumor necroptosis in breast cancer. Nat Commun 12:2666. https://doi.org/10.1038/s41467-021-23004-3

Caccamo A, Branca C, Piras IS, Ferreira E, Huentelman MJ, Liang WS, Readhead B, Dudley JT, Spangenberg EE, Green KN, Belfiore R, Winslow W, Oddo S (2017) Necroptosis activation in Alzheimer's disease. Nat Neurosci 20:1236–1246. https://doi.org/10.1038/nn.4608

Chen J, Kos R, Garssen J, Redegeld F (2019) Molecular insights into the mechanism of necroptosis: the necrosome as a potential therapeutic target. Cells 8:1. https://doi.org/10.3390/cells8121486

Christgen S, Zheng M, Kesavardhana S, Karki R, Malireddi R, Banoth B, Place DE, Briard B, Sharma BR, Tuladhar S, Samir P, Burton A, Kanneganti TD (2020) Identification of the PANoptosome: a molecular platform triggering pyroptosis, apoptosis, and necroptosis (PANoptosis). Front Cell Infect Microbiol 10:237. https://doi.org/10.3389/fcimb.2020.00237

Devos M, Tanghe G, Gilbert B, Dierick E, Verheirstraeten M, Nemegeer J, de Reuver R, Lefebvre S, De Munck J, Rehwinkel J, Vandenabeele P, Declercq W, Maelfait J (2020) Sensing of endogenous nucleic acids by ZBP1 induces keratinocyte necroptosis and skin inflammation. J Exp Med 217:1. https://doi.org/10.1084/jem.20191913

Farber E (1994) Programmed cell death: necrosis versus apoptosis. Mod Pathol 7:605–609

Fritsch M, Günther SD, Schwarzer R, Albert MC, Schorn F, Werthenbach JP, Schiffmann LM, Stair N, Stocks H, Seeger JM, Lamkanfi M, Krönke M, Pasparakis M, Kashkar H (2019) Caspase-8 is the molecular switch for apoptosis, necroptosis and pyroptosis. Nature 575:683–687. https://doi.org/10.1038/s41586-019-1770-6

Galluzzi L, Kroemer G (2008) Necroptosis: a specialized pathway of programmed necrosis. Cell 135:1161–1163. https://doi.org/10.1016/j.cell.2008.12.004

Garcia LR, Tenev T, Newman R, Haich RO, Liccardi G, John SW, Annibaldi A, Yu L, Pardo M, Young SN, Fitzgibbon C, Fernando W, Guppy N, Kim H, Liang LY, Lucet IS, Kueh A, Roxanis I, Gazinska P, Sims M, Smyth T, Ward G, Bertin J, Beal AM, Geddes B, Choudhary JS, Murphy JM, Aurelia BK, Upton JW, Meier P (2021) Ubiquitylation of MLKL at lysine 219 positively regulates necroptosis-induced tissue injury and pathogen clearance. Nat Commun 12:3364. https://doi.org/10.1038/s41467-021-23474-5

Gurung P, Anand PK, Malireddi RK, Vande WL, Van Opdenbosch N, Dillon CP, Weinlich R, Green DR, Lamkanfi M, Kanneganti TD (2014) FADD and caspase-8 mediate priming and activation of the canonical and noncanonical Nlrp3 inflammasomes. J Immunol 192:1835–1846. https://doi.org/10.4049/jimmunol.1302839

Ha SC, Van Quyen D, Hwang HY, Oh DB, Brown BN, Lee SM, Park HJ, Ahn JH, Kim KK, Kim YG (2006) Biochemical characterization and preliminary X-ray crystallographic study of the domains of human ZBP1 bound to left-handed Z-DNA. Biochim Biophys Acta 1764:320–323. https://doi.org/10.1016/j.bbapap.2005.12.012

Ha SC, Kim D, Hwang HY, Rich A, Kim YG, Kim KK (2008) The crystal structure of the second Z-DNA binding domain of human DAI (ZBP1) in complex with Z-DNA reveals an unusual binding mode to Z-DNA. Proc Natl Acad Sci USA 105:20671–20676. https://doi.org/10.1073/pnas.0810463106

Henry CM, Martin SJ (2017) Caspase-8 acts in a non-enzymatic role as a scaffold for assembly of a pro-inflammatory "FADDosome" complex upon TRAIL stimulation. Mol Cell 65:715–729. https://doi.org/10.1016/j.molcel.2017.01.022

Iannielli A, Bido S, Folladori L, Segnali A, Cancellieri C, Maresca A, Massimino L, Rubio A, Morabito G, Caporali L, Tagliavini F, Musumeci O, Gregato G, Bezard E, Carelli V, Tiranti V, Broccoli V (2018) Pharmacological inhibition of necroptosis protects from dopaminergic neuronal cell death in Parkinson's disease models. Cell Rep 22:2066–2079. https://doi.org/10.1016/j.celrep.2018.01.089

Ingram JP, Thapa RJ, Fisher A, Tummers B, Zhang T, Yin C, Rodriguez DA, Guo H, Lane R, Williams R, Slifker MJ, Basagoudanavar SH, Rall GF, Dillon CP, Green DR, Kaiser WJ, Balachandran S (2019) ZBP1/DAI drives RIPK3-mediated cell death induced by IFNs in the absence of RIPK1. J Immunol 203:1348–1355. https://doi.org/10.4049/jimmunol.1900216

Ito Y, Ofengeim D, Najafov A, Das S, Saberi S, Li Y, Hitomi J, Zhu H, Chen H, Mayo L, Geng J, Amin P, DeWitt JP, Mookhtiar AK, Florez M, Ouchida AT, Fan JB, Pasparakis M, Kelliher MA, Ravits J, Yuan J (2016) RIPK1 mediates axonal degeneration by promoting inflammation and necroptosis in ALS. Science 353:603–608. https://doi.org/10.1126/science.aaf6803

Jiao H, Wachsmuth L, Kumari S, Schwarzer R, Lin J, Eren RO, Fisher A, Lane R, Young GR, Kassiotis G, Kaiser WJ, Pasparakis M (2020) Z-nucleic-acid sensing triggers ZBP1-dependent necroptosis and inflammation. Nature 580:391–395. https://doi.org/10.1038/s41586-020-2129-8

Jin Q, Li T, He X, Jia H, Chen G, Zeng S, Fang Y, Jing Z, Yang X (2015) Molecular structural characteristics and the functions of mouse DNA-dependent activator of interferon-regulatory factors. Xi Bao Yu Fen Zi Mian Yi Xue Za Zhi 31:1606–1610

Kaiser WJ, Offermann MK (2005) Apoptosis induced by the toll-like receptor adaptor TRIF is dependent on its receptor interacting protein homotypic interaction motif. J Immunol 174:4942–4952. https://doi.org/10.4049/jimmunol.174.8.4942

Kaiser WJ, Upton JW, Mocarski ES (2008) Receptor-interacting protein homotypic interaction motif-dependent control of NF-kappa B activation via the DNA-dependent activator of IFN regulatory factors. J Immunol 181:6427–6434. https://doi.org/10.4049/jimmunol.181.9.6427

Kaiser WJ, Sridharan H, Huang C, Mandal P, Upton JW, Gough PJ, Sehon CA, Marquis RW, Bertin J, Mocarski ES (2013) Toll-like receptor 3-mediated necrosis via TRIF, RIP3, and MLKL. J Biol Chem 288:31268–31279. https://doi.org/10.1074/jbc.M113.462341

Kamiya M, Mizoguchi F, Kawahata K, Wang D, Nishibori M, Day J, Louis C, Wicks IP, Kohsaka H, Yasuda S (2022) Targeting necroptosis in muscle fibers ameliorates inflammatory myopathies. Nat Commun 13:166. https://doi.org/10.1038/s41467-021-27875-4

Karki R, Lee S, Mall R, Pandian N, Wang Y, Sharma BR, Malireddi RS, Yang D, Trifkovic S, Steele JA, Connelly JP, Vishwanath G, Sasikala M, Reddy DN, Vogel P, Pruett-Miller SM, Webby R, Jonsson CB, Kanneganti TD (2022) ZBP1-dependent inflammatory cell death, PANoptosis, and cytokine storm disrupt IFN therapeutic efficacy during coronavirus infection. Sci Immunol 7:o6294. https://doi.org/10.1126/sciimmunol.abo6294

Karunakaran D, Geoffrion M, Wei L, Gan W, Richards L, Shangari P, DeKemp EM, Beanlands RA, Perisic L, Maegdefessel L, Hedin U, Sad S, Guo L, Kolodgie FD, Virmani R, Ruddy T, Rayner KJ (2016) Targeting macrophage necroptosis for therapeutic and diagnostic interventions in atherosclerosis. Sci Adv 2:e1600224. https://doi.org/10.1126/sciadv.1600224

Kesavardhana S, Malireddi R, Burton AR, Porter SN, Vogel P, Pruett-Miller SM, Kanneganti TD (2020) The Zα2 domain of ZBP1 is a molecular switch regulating influenza-induced PANoptosis and perinatal lethality during development. J Biol Chem 295:8325–8330. https://doi.org/10.1074/jbc.RA120.013752

Khoury MK, Gupta K, Franco SR, Liu B (2020) Necroptosis in the pathophysiology of disease. Am J Pathol 190:272–285. https://doi.org/10.1016/j.ajpath.2019.10.012

Kuriakose T, Man SM, Malireddi RK, Karki R, Kesavardhana S, Place DE, Neale G, Vogel P, Kanneganti TD (2016) ZBP1/DAI is an innate sensor of influenza virus triggering the NLRP3 inflammasome and programmed cell death pathways. Sci Immunol 1:1. https://doi.org/10.1126/sciimmunol.aag2045

Li D, Meng L, Xu T, Su Y, Liu X, Zhang Z, Wang X (2017) RIPK1-RIPK3-MLKL-dependent necrosis promotes the aging of mouse male reproductive system. Elife 6:1. https://doi.org/10.7554/eLife.27692

Lin QS, Chen P, Wang WX, Lin CC, Zhou Y, Yu LH, Lin YX, Xu YF, Kang DZ (2020) RIP1/RIP3/MLKL mediates dopaminergic neuron necroptosis in a mouse model of Parkinson disease. Lab Invest 100:503–511. https://doi.org/10.1038/s41374-019-0319-5

Malireddi R, Kesavardhana S, Kanneganti TD (2019) ZBP1 and TAK1: master regulators of NLRP3 inflammasome/pyroptosis, apoptosis, and necroptosis (PAN-optosis). Front Cell Infect Microbiol 9:406. https://doi.org/10.3389/fcimb.2019.00406

Man SM, Tourlomousis P, Hopkins L, Monie TP, Fitzgerald KA, Bryant CE (2013) Salmonella infection induces recruitment of Caspase-8 to the inflammasome to modulate IL-1β production. J Immunol 191:5239–5246. https://doi.org/10.4049/jimmunol.1301581

Martens S, Bridelance J, Roelandt R, Vandenabeele P, Takahashi N (2021) MLKL in cancer: more than a necroptosis regulator. Cell Death Differ 28:1757–1772. https://doi.org/10.1038/s41418-021-00785-0

Meng L, Jin W, Wang X (2015) RIP3-mediated necrotic cell death accelerates systematic inflammation and mortality. Proc Natl Acad Sci USA 112:11007–11012. https://doi.org/10.1073/pnas.1514730112

Mishra PK, Adameova A, Hill JA, Baines CP, Kang PM, Downey JM, Narula J, Takahashi M, Abbate A, Piristine HC, Kar S, Su S, Higa JK, Kawasaki NK, Matsui T (2019) Guidelines for evaluating myocardial cell death. Am J Physiol Heart Circ Physiol 317:H891–H922. https://doi.org/10.1152/ajpheart.00259.2019

Mizumura K, Maruoka S, Gon Y, Choi AM, Hashimoto S (2016) The role of necroptosis in pulmonary diseases. Respir Investig 54:407–412. https://doi.org/10.1016/j.resinv.2016.03.008

Moore KJ, Tabas I (2011) Macrophages in the pathogenesis of atherosclerosis. Cell 145:341–355. https://doi.org/10.1016/j.cell.2011.04.005

Muendlein HI, Connolly WM, Magri Z, Smirnova I, Ilyukha V, Gautam A, Degterev A, Poltorak A (2021) ZBP1 promotes LPS-induced cell death and IL-1β release via RHIM-mediated interactions with RIPK1. Nat Commun 12:86. https://doi.org/10.1038/s41467-020-20357-z

Murphy JM, Czabotar PE, Hildebrand JM, Lucet IS, Zhang JG, Alvarez-Diaz S, Lewis R, Lalaoui N, Metcalf D, Webb AI, Young SN, Varghese LN, Tannahill GM, Hatchell EC, Majewski IJ, Okamoto T, Dobson RC, Hilton DJ, Babon JJ, Nicola NA, Strasser A, Silke J, Alexander WS (2013) The pseudokinase MLKL mediates necroptosis via a molecular switch mechanism. Immunity 39:443–453. https://doi.org/10.1016/j.immuni.2013.06.018

Newton K, Wickliffe KE, Maltzman A, Dugger DL, Strasser A, Pham VC, Lill JR, Roose-Girma M, Warming S, Solon M, Ngu H, Webster JD, Dixit VM (2016) RIPK1 inhibits ZBP1-driven necroptosis during development. Nature 540:129–133. https://doi.org/10.1038/nature20559

Ofengeim D, Yuan J (2013) Regulation of RIP1 kinase signalling at the crossroads of inflammation and cell death. Nat Rev Mol Cell Biol 14:727–736. https://doi.org/10.1038/nrm3683

Oñate M, Catenaccio A, Salvadores N, Saquel C, Martinez A, Moreno-Gonzalez I, Gamez N, Soto P, Soto C, Hetz C, Court FA (2020) The necroptosis machinery mediates axonal degeneration in a model of Parkinson disease. Cell Death Differ 27:1169–1185. https://doi.org/10.1038/s41418-019-0408-4

Pearson JS, Giogha C, Mühlen S, Nachbur U, Pham CL, Zhang Y, Hildebrand JM, Oates CV, Lung TW, Ingle D, Dagley LF, Bankovacki A, Petrie EJ, Schroeder GN, Crepin VF, Frankel G, Masters SL, Vince J, Murphy JM, Sunde M, Webb AI, Silke J, Hartland EL (2017) EspL is a bacterial cysteine protease effector that cleaves RHIM proteins to block necroptosis and inflammation. Nat Microbiol 2:16258. https://doi.org/10.1038/nmicrobiol.2016.258

Peltzer N, Darding M, Montinaro A, Draber P, Draberova H, Kupka S, Rieser E, Fisher A, Hutchinson C, Taraborrelli L, Hartwig T, Lafont E, Haas TL, Shimizu Y, Böiers C, Sarr A, Rickard J, Alvarez-Diaz S, Ashworth MT, Beal A, Enver T, Bertin J, Kaiser W, Strasser A, Silke J, Bouillet P, Walczak H (2018) LUBAC is essential for embryogenesis by preventing cell death and enabling haematopoiesis. Nature 557:112–117. https://doi.org/10.1038/s41586-018-0064-8

Peng QL, Zhang YM, Liu YC, Liang L, Li WL, Tian XL, Zhang L, Yang HX, Lu X, Wang GC (2022) Contribution of necroptosis to Myofiber death in idiopathic inflammatory myopathies. Arthritis Rheumatol 74:1048–1058. https://doi.org/10.1002/art.42071

Rebsamen M, Heinz LX, Meylan E, Michallet MC, Schroder K, Hofmann K, Vazquez J, Benedict CA, Tschopp J (2009) DAI/ZBP1 recruits RIP1 and RIP3 through RIP homotypic interaction motifs to activate NF-kappaB. EMBO Rep 10:916–922. https://doi.org/10.1038/embor.2009.109

Rodriguez DA, Weinlich R, Brown S, Guy C, Fitzgerald P, Dillon CP, Oberst A, Quarato G, Low J, Cripps JG, Chen T, Green DR (2016) Characterization of RIPK3-mediated phosphorylation of the activation loop of MLKL during necroptosis. Cell Death Differ 23:76–88. https://doi.org/10.1038/cdd.2015.70

Salvadores N, Moreno-Gonzalez I, Gamez N, Quiroz G, Vegas-Gomez L, Escandón M, Jimenez S, Vitorica J, Gutierrez A, Soto C, Court FA (2022) Aβ oligomers trigger necroptosis-mediated neurodegeneration via microglia activation in Alzheimer's disease. Acta Neuropathol Commun 10:31. https://doi.org/10.1186/s40478-022-01332-9

Samir P, Malireddi R, Kanneganti TD (2020) The PANoptosome: a deadly protein complex driving pyroptosis, apoptosis, and necroptosis (PANoptosis). Front Cell Infect Microbiol 10:238. https://doi.org/10.3389/fcimb.2020.00238

Schwarzer R, Laurien L, Pasparakis M (2020) New insights into the regulation of apoptosis, necroptosis, and pyroptosis by receptor interacting protein kinase 1 and caspase-8. Curr Opin Cell Biol 63:186–193. https://doi.org/10.1016/j.ceb.2020.02.004

Udawatte DJ, Rothman AL (2021) Viral Suppression of RIPK1-Mediated Signaling. mBio 12: e172321. https://doi.org/10.1128/mBio.01723-21.

Wang Y, Kanneganti TD (2021) From pyroptosis, apoptosis and necroptosis to PANoptosis: a mechanistic compendium of programmed cell death pathways. Comput Struct Biotechnol J 19:4641–4657. https://doi.org/10.1016/j.csbj.2021.07.038

Wang Z, Choi MK, Ban T, Yanai H, Negishi H, Lu Y, Tamura T, Takaoka A, Nishikura K, Taniguchi T (2008) Regulation of innate immune responses by DAI (DLM-1/ZBP1) and other DNA-sensing molecules. Proc Natl Acad Sci USA 105:5477–5482. https://doi.org/10.1073/pnas.0801295105

Xia X, Lei L, Wang S, Hu J, Zhang G (2020) Necroptosis and its role in infectious diseases. Apoptosis 25:169–178. https://doi.org/10.1007/s10495-019-01589-x

Xue C, Gu X, Li G, Bao Z, Li L (2020) Mitochondrial mechanisms of necroptosis in liver diseases. Int J Mol Sci 22:1. https://doi.org/10.3390/ijms22010066

Zhan C, Huang M, Yang X, Hou J (2021) MLKL: functions beyond serving as the executioner of necroptosis. Theranostics 11:4759–4769. https://doi.org/10.7150/thno.54072